



RESEARCH ARTICLE

# Exercise-induced loading increases ilium cortical area in a selectively bred mouse model

Kristi L. Lewton<sup>1,2,3</sup>  | Terrence Ritzman<sup>4,5,6</sup> | Lynn E. Copes<sup>7</sup>  | Theodore Garland Jr<sup>8</sup> | Terence D. Capellini<sup>3</sup>

<sup>1</sup>Department of Integrative Anatomical Sciences, Keck School of Medicine, University of Southern California, Los Angeles, CA

<sup>2</sup>Department of Biological Sciences, Human & Evolutionary Biology Section, University of Southern California, Los Angeles, CA

<sup>3</sup>Department of Human Evolutionary Biology, Harvard University, Cambridge, MA

<sup>4</sup>Department of Neuroscience, Washington University School of Medicine, St. Louis, MO

<sup>5</sup>Department of Anthropology, Washington University, St. Louis, MO

<sup>6</sup>Human Evolution Research Institute, University of Cape Town, Cape Town, South Africa

<sup>7</sup>Department of Medical Sciences, Frank H. Netter MD School of Medicine, Quinnipiac University, Hamden, CT

<sup>8</sup>Department of Evolution, Ecology, and Organismal Biology, University of California, Riverside, Riverside, CA

## Correspondence

Kristi L. Lewton, University of Southern California, Keck School of Medicine, Department of Integrative Anatomical Sciences.  
Email: kristilewton@gmail.com

## Funding information

Division of Behavioral and Cognitive Sciences, Grant/Award Number: 0925793; Division of Environmental Biology, Grant/Award Number: 1655362; Division of Integrative Organismal Systems, Grant/Award Number: 11212732; Wenner-Gren Foundation, Grant/Award Number: 8102

## Abstract

**Objectives:** Little is known about how ilium cortical bone responds to loading. Using a mouse model, this study presents data testing the hypothesis that iliac cross-sectional properties are altered in response to increased activity.

**Materials and Methods:** The sample derives from lines of High Runner (HR) mice bred for increased wheel-running activity. Four treatment groups of female mice were tested: non-selected control lines housed without ( $N = 19$ ) and with wheels ( $N = 20$ ), and HR mice housed without ( $N = 17$ ) and with wheels ( $N = 18$ ) for 13 weeks beginning at weaning. Each pelvis was  $\mu$ CT-scanned, cross-sectional properties (cortical area— $Ct.Ar$ , total area— $Tt.Ar$ , polar moment of area, and polar section modulus) were determined from the ilium midshaft, and robusticity indices (ratio of the square root of  $Ct.Ar$  or  $Tt.Ar$  to caudal ilium length) were calculated. Mixed models were implemented with linetype, wheel access, and presence of the mini-muscle phenotype as fixed effects, replicate line nested within linetype as a random effect, and body mass as a covariate.

**Results:** Results demonstrate that the mouse ilium morphologically resembles a long bone in cross section. Body mass and the mini-muscle phenotype were significant predictors of iliac cross-sectional properties. Wheel access only had a statistically significant effect on  $Ct.Ar$  and its robusticity index, with greater values in mice with wheel access.

**Discussion:** These results suggest that voluntary exercise increases cortical area, but does not otherwise strengthen the ilium in these mice, corroborating previous studies on the effect of increased wheel-running activity on femoral and humeral cross-sectional properties in these mice.

## KEYWORDS

bone biology, cross-sectional geometry, mouse, pelvis, running

## 1 | INTRODUCTION

The pelvic girdle is an integral component of the hindlimb locomotor system, with roles in muscle attachment and force transmission. Force transmission from the hindlimb to the torso occurs through the caudal ilium, the beam-like region between the sacroiliac and coxal joints (Dalstra & Huiskes, 1995). As a result, the bony morphology of the caudal ilium is expected to exhibit adaptations to hindlimb locomotor

loading, especially in taxa that experience relatively large hindlimb loads such as bipeds and leapers. Recent work in strepsirrhine primates has shown that caudal ilium cross-sectional area is relatively larger in species that encounter large locomotor loads relative to body mass (Lewton, 2015c). In addition to the effects of locomotor loading on ilium morphology, scaling analyses across haplorhine and strepsirrhine primates demonstrate allometry of caudal ilium robusticity dimensions (i.e., caudal ilium length scales with negative allometry and

cross-sectional area scales with positive allometry). Together, these data support the hypothesis that a short, wide caudal ilium has evolved in concert with large loads resulting from locomotion and increases in body mass (Lewton, 2015a). It remains unresolved whether this association between caudal ilium morphology and locomotor behavior is the result of genetic differences among species that differ in habitual loading regimes, the result of bone functional adaptation (i.e., skeletal adaptation within an individual's lifetime), or more likely, the result of a combination of genetic and behavioral adaptation. Furthermore, how internal ilium bone morphology—cross-sectional geometric properties—responds to varied loading conditions is unknown.

Data on the dynamic responses to loading are critical for understanding how the pelvis adapts to the loads it encounters, and ultimately, for attempts to reconstruct locomotor adaptation in the fossil record. Experimental work that varies loading conditions in the pelvis of primates pushes the limits of feasibility, but a mouse model has proven useful for understanding bone biology and biomechanics for other parts of the skeletal system, such as semicircular canals (Schutz, Jamniczky, Hallgrímsson, & Garland Jr., 2014) and hindlimb bones (Kelly, Czech, Wight, Blank, & Garland Jr., 2006; Wallace et al., 2010; Wallace, Tommasini, Judex, Garland Jr., & Demes, 2012). The primary aim of this study is to examine cross-sectional geometric properties in the caudal ilium of mice that have experienced increased physical activity on running wheels from weaning and on through adulthood as compared to a control sample housed without wheels.

Diaphyseal cross-sectional geometric properties can reflect bone loading history. Studies of long bone cross-sectional geometric properties have correlated bone strength to locomotor loading in humans and nonhuman primates (e.g., Burr, Piotrowski, Martin, & Cook, 1982; Burr, Ruff, & Johnson, 1989; Carlson, 2005; Demes & Jungers, 1993; Marchi, 2007; Patel, Ruff, Simons, & Organ, 2013; Ruff, 2002, 2003; Schaffler, Burr, Jungers, & Ruff, 1985) and to human mobility and activity patterns (e.g., Carlson & Marchi, 2014; Pearson, 2000; Ruff & Hayes, 1983; Shaw & Stock, 2009; Stock & Pfeiffer, 2001; Trinkaus & Churchill, 1999; Trinkaus, Ruff, Churchill, & Vandermeersch, 1998).

Comparative studies of nonhuman primate long bone cross-sectional geometry demonstrate evolutionary adaptations to locomotion such as leaping versus nonleaping behaviors. Cortical area ( $Ct.Ar$ , an estimator of compressive strength) is greater in femora than in humeri in quadrupedal primates, and this difference is more pronounced in leaping versus nonleaping species (Demes & Jungers, 1993; Terranova, 1995a, 1995b). Similarly, bones that experience larger loads may exhibit greater  $Ct.Ar$ ; in quadrupedal primates,  $Ct.Ar$  is larger in tibiae than ulnae (Demes et al., 1998; Demes, Qin, Stern, Larson, & Rubin, 2001). The distribution of cortical bone in a cross section provides information about bone torsional ( $J$ , polar second moment of area) and bending strengths ( $I$  and  $Z_p$ , moment of inertia and polar section modulus, respectively), as well as the directions of greatest bone strength. In small-bodied leaping strepsirrhines (i.e., galagos), the femur demonstrates larger  $I$  values in the anteroposterior direction ( $I_{AP}$ ) relative to the mediolateral direction ( $I_{ML}$ ), which suggests that it has greatest resistance to bending in the anteroposterior plane (Burr et al., 1982; Demes & Jungers, 1993; Terranova, 1995a, 1995b). Quadrupedal galagos, conversely, demonstrate similar

femoral  $I_{AP}$  and  $I_{ML}$  values, indicating similar resistance to bending in the anteroposterior and mediolateral directions (Terranova, 1995a, 1995b). Although research on bone cross-sectional geometry has led to inferences about bone adaptations to locomotor loading patterns, experimental studies have shown that the correlation between loading regimes (strain magnitudes and orientations) and cross-sectional properties is inconsistent, and sometimes these variables yield conflicting results (Demes et al., 1998, 2001; Lieberman & Pearson, 2001; Lieberman, Polk, & Demes, 2004; Pearson & Lieberman, 2004).

In comparison to research on limb bones, relatively little work has examined bone biomechanics and microarchitecture of the pelvic girdle. The vast majority of studies on pelvic bone biomechanics has focused on clinical questions related to human hip and pelvic fractures, and more commonly, hip joint replacements (Carter, Vasu, & Harris, 1982; Finlay, Bourne, Landsberg, & Andreae, 1986; Huiskes, 1987; Linstrom et al., 2009; Lionberger, Walker, & Granholm, 1985; Ries, Pugh, Au, Gurtowski, & Dee, 1989; Shim, Pitto, Streicher, Hunter, & Anderson, 2007). This clinical work has shown that stresses are transmitted from the hip joint to the sacroiliac joint via the lower ilium (Dalstra & Huiskes, 1995). Principal strains collected from cadaveric specimens reflect this transmission pathway and are primarily oriented craniocaudally in both humans (Ries et al., 1989) and nonhuman primates (Lewton, 2015b). Clinical research has not examined cortical bone parameters of the lower ilium, instead focusing on whole-bone finite element analyses, bone mineral density analyses of the iliac crest, and direct studies of the lunatic surface of the acetabulum for improving prosthetic devices such as acetabulum implants (e.g., Anderson, Peters, Tuttle, & Weiss, 2005; Dalstra, Huiskes, & van Erning, 1995; Misof et al., 2014; Roschger, Paschalis, Fratzl, & Klaushofer, 2008). Therefore, how ilium cross-sectional geometry may be related to loading patterns remains unknown.

Quantifying the typical loading environment of the primate pelvis is challenging because the pelvic girdle is wholly encased in hindlimb musculature, making it difficult to collect strain gauge data (Lewton, 2015b). In addition, comparing loading versus non-loading experimental conditions is difficult in primates because it requires preventing the use of a limb, and does not easily allow for testing the effects of increased loads. One way around this difficulty has been to use mice as models in studies of primate bone biology because it is feasible to manipulate their loading environments through various types of forced or voluntary exercise (e.g., Copes et al., 2015; Copes, Schutz, Dlugosz, Judex, & Garland Jr., 2018; Green, Richmond, & Miran, 2012; Wallace et al., 2012). In this study, we test the hypothesis that increased physical activity results in ilium cross-sectional properties that are indicative of greater resistance to loading. To increase power to detect such exercise-training effects, we used mice from four replicate lines that have been selectively bred for high levels of voluntary wheel running than their four nonselected control lines (Swallow, Carter, & Garland Jr., 1998; Wallace & Garland Jr., 2016). Inclusion of the nonselected control lines allows the opportunity to test for genotype-by-environment interactions. To the best of our knowledge, our study is the first to qualitatively and quantitatively describe the internal morphology of the beam-like caudal ilium of the mouse.

## 2 | MATERIALS AND METHODS

### 2.1 | Sample

The mice used in this study derive from a starting sample of 112 male and 112 female mice from the outbred Hsd:ICR mouse strain that were selectively bred for high voluntary exercise for 57 generations in the laboratory of Theodore Garland starting in 1993. After two generations of random mating, mice were randomly assigned to one of eight lines; four lines were selectively bred for increased voluntary wheel running activity (HR), and four lines were designated as controls (Swallow et al., 1998). Mice have been continuously randomly bred within the control lines since the start of the original experiment (with a prohibition on sibling mating). HR mice were given access to wheels for 6 days when they were ~6–8 weeks old. Their total running on days 5 and 6 were averaged, and the mice with the highest values were bred with one another using a within-family selection scheme (with a prohibition on sibling mating). Wheel running activity was recorded via revolution data from a photocell counter affixed to the wheel and collected daily at 1-min intervals (Copes et al., 2015; Swallow et al., 1998).

In three of the eight original lines of mice used here, a mini-muscle phenotype occurred with low frequency in one of the control lines and ~50% frequency in two of the selected lines when first reported at generation 22 (Garland Jr. et al., 2002). The mini-muscle phenotype is associated with ~50% decreased *m. triceps surae* and total hindlimb muscle mass, and is caused by a Mendelian recessive single nucleotide polymorphism in the intron of a myosin heavy chain gene (Kelly et al., 2013). Population genetic modeling showed that this phenotype had been favored (unintentionally) by the selection regimen. By the time of the present sample at generation 57, the phenotype had disappeared from the control line, became fixed in one HR line (lab designation #3), and remained polymorphic in another HR line (#6). The mini-muscle gene and phenotype is, therefore, an important part of the adaptive response to the selection regime, and serves as an illustration of novel and unexpected multiple responses to selection (Garland Jr. et al., 2002; Garland Jr. et al., 2011; Garland Jr., 2003). The mini-muscle phenotype is associated with a variety of differences in bone dimensions and mechanical properties (Castro & Garland Jr., 2018; Kelly et al., 2006; Middleton et al., 2010; Middleton, Kelly, & Garland Jr., 2008; Peacock, Garland Jr., & Middleton, 2018; Schwartz, Patel, Garland Jr., & Horner, 2018). Thus, we were also interested in the effects of decreased muscularity (and possibly other pathways for pleiotropic effects) on bone properties.

This study uses a two-way experimental design, in which female HR and control mice ( $N = 74$ ) from the 57th generation were divided into four experimental groups at weaning based on access to a running wheel attached to individual housing cages (i.e., each mouse was housed in its own cage; these are the same individuals included in Copes et al., 2015, 2018). Thus, mice were assigned to one of four experimental groups: control mice without access to a wheel ( $N = 19$ ), control mice with access to a wheel ( $N = 20$ ), HR mice without access to a wheel ( $N = 17$ ), and HR mice with access to a wheel ( $N = 18$ ). Mice were provided with food (Teklad Harlan 8604 pellet diet) and water ad libitum. This experimental design is uniquely situated to

differentiate evolved differences from individual-level differences (i.e., bone functional adaptation). A 12-week experiment on this sample of mice collected data on total wheel revolutions, daily minutes of activity, mean running speed, and maximum speed, and has shown that HR mice with wheel access ran for significantly greater distances, duration, and at higher mean speeds than control mice with wheel access (Copes et al., 2015; Copes et al., 2018). These variables were analyzed at week eight and the results demonstrate that HR mice ran 2.31 times farther, 1.31 times as long, and 1.91 times faster (average speed) than control mice (Copes et al., 2015). In addition to wheel-running activity, all physical activity within the home cage, regardless of wheel access, was collected daily via infrared motion detection sensors and summed over a 23.5 hr period (Copes et al., 2018). In this sample of mice, HR mice without wheel access exhibited significantly greater total home cage activity (1.5 times greater) than control mice without wheel access (Copes et al., 2015). Total home cage activity did not significantly differ between HR and control mice with access to wheels (Copes et al., 2015).

Mice were culled at 15 weeks of age, and body mass at death was recorded. Bones were cleaned and prepared by LEC by soaking each carcass in a solution of Tergazyme enzymatic cleaner, which was changed every 24 hr. Over the course of approximately 10 days, the soft tissue dissolved, leaving the bones clean for analysis. All experimental procedures were approved by the Institutional Animal Care and Use Committee of the University of California, Riverside.

### 2.2 | $\mu$ CT imaging and calculation of cross-sectional geometric properties

The right os coxae of each mouse was  $\mu$ CT scanned on a Nikon X-Tek HMXST225 scanner at the Harvard University Center for Nanoscale Systems. In cases where the right os coxae was damaged, the left os coxae was scanned instead and later digitally mirrored. Ossa coxae were mounted in floral foam (10–12 specimens per piece of foam) and scanned at resolutions ranging from ~12–15  $\mu$ m using a Perkin Elmer 1621 2000 by 2000 pixel detector. Scan energy settings were 70 kV and 165  $\mu$ A, and no filter was used. Scans were reconstructed using CT Pro 3D software and exported as 16-bit TIFF images.

Each os coxae model was individually segmented and, if necessary, digitally mirror-imaged to represent the right side, and aligned using a standardized protocol in Avizo Lite v. 9.0.1 software. Models were aligned such that the ilium was superior, the ischium inferior, and the pubic symphysis and auricular surface faced medially. The ilium was oriented vertically so that cross sections through it would be orthogonal to the long axis of the bone. The Align Principal Axes module was applied to the surface model of the data, which orients the model according to its principal axes, and results in alignment that is close to proper anatomical position and requires minor adjustments from the user. The model was rotated using the Transform Editor to ensure that the XY plane was oriented transversely, showing the ischiopubic region, the XZ plane was oriented coronally, showing the ventral aspect of the bone, and the YZ plane was oriented sagittally, showing the medial aspect of the bone. The Scan Surface to Volume module was applied to the reoriented data to convert the surface model to a volumetric model. To delineate the caudal ilium segment,

three orthoslices were applied to the volume, manually positioned at the superior, middle, and inferior aspects of the caudal ilium. The superior extent of the caudal ilium was defined as the inferior-most aspect of the auricular surface. The inferior extent of the caudal ilium was defined as the superior-most aspect of the acetabular rim. The middle of the caudal ilium was the slice located at 50% the distance between the superior and inferior caudal ilium slices (Figure 1). To approximate midshaft cross-sectional geometry similar to those obtained on studies of long bones, the 50% caudal ilium slice was exported as a DICOM image for cross-sectional geometry analysis using the BoneJ plugin (Doubé et al., 2010) for ImageJ software (Schneider, Rasband, & Eliceiri, 2012).

Cross-sectional geometric properties—cortical area (Ct.Ar, a measure of compressive strength), total cross-sectional area

(periosteal area, Tt.Ar), and polar section modulus ( $Z_p$ , a measure of bending strength) were calculated using the Slice Geometry tool in BoneJ. Polar moment of area ( $J$ ), a measure of torsional strength, was calculated as the sum of the maximum and minimum second moments of area. To evaluate the relative robusticity of the caudal ilium, two robusticity indices were calculated as the ratio of the square root of either Ct.Ar or Tt.Ar to caudal ilium length (IL, the distance between the superior and inferior caudal ilium slices).

## 2.3 | Statistical analysis

To determine the effects of selective breeding and wheel access on caudal ilium cross-sectional geometric properties, mixed effects model analyses of covariance (ANCOVA) were performed with the following

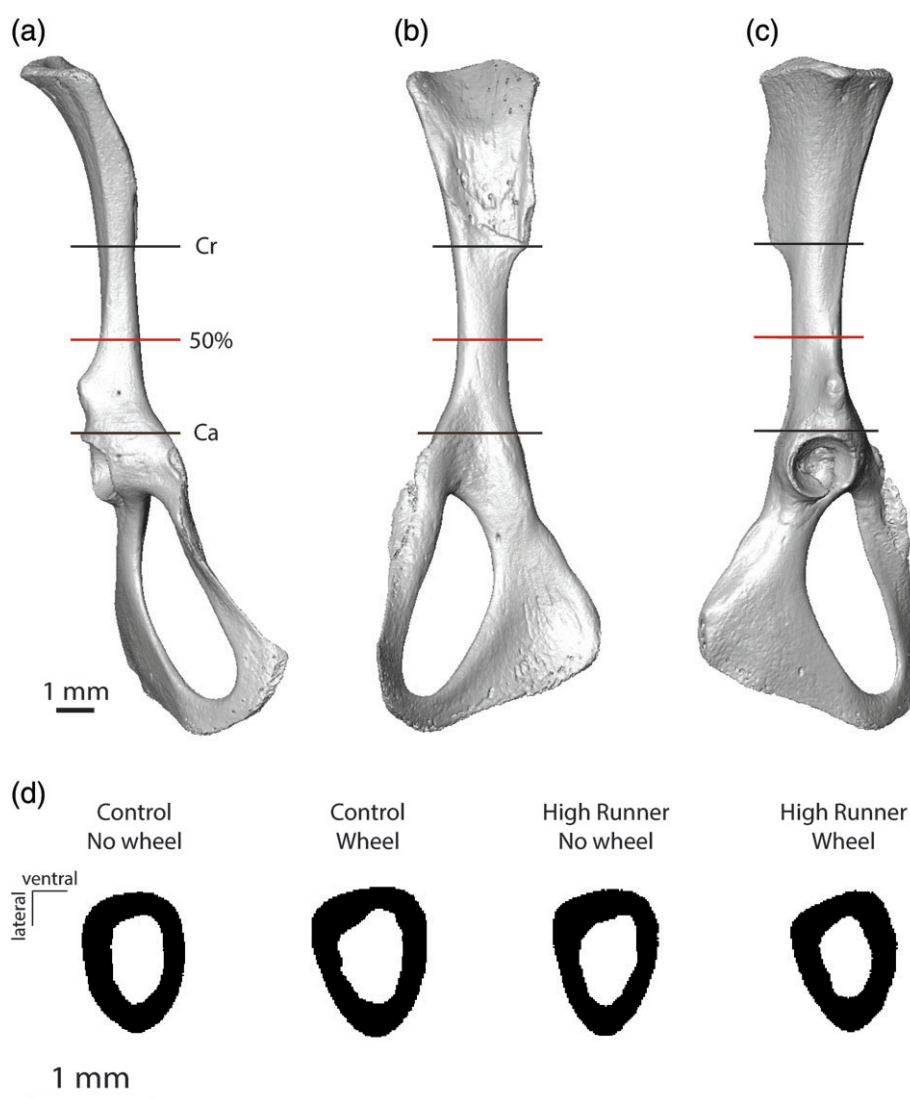


**FIGURE 1** Locations of the 50% midshaft slice in ventral (a), medial (b) and lateral (c) views of specimen 339, an individual from the control group without access to a wheel. The 50% slice is half the distance between the cranial (Cr) and caudal (Ca) aspects of the caudal ilium (see Methods for more details). Representative cross-sections for each treatment group are shown in (d). specimen identification numbers from left to right are 344, 275, 348, 314 (corresponding raw cortical area values are 0.57, 0.61, 0.56, and 0.56 mm<sup>2</sup>). None of the HR individuals in (d) derive from lines in which the mini-muscle phenotype is present. Cortical area means are absolutely larger in the control lines compared to the HR lines (Table 1, raw means); this pattern diminishes when body mass is included as a covariate in the ANCOVA (Table 3, least-squares means)

fixed effects: linetype (selected vs control), activity (wheel access), the interaction of linetype and activity, presence of the mini-muscle phenotype, and body mass. Replicate line was nested as a random effect within linetype. Degrees of freedom (d.f) for effects of linetype, wheel access, and their interaction were nominally 1 and 6. However, missing data reduced this to 1 and 5 d.f. For testing effects of the mini-muscle phenotype and of body mass relative to the residual variance, d.f. were 1 and 56 or 57. We also ran models that included the interaction between activity and mini-muscle status to test whether mini-muscle individuals responded similarly to wheel access as compared with normal-muscled individuals. In no case did this term approach statistical significance (all  $p > .77$ ), so these models are not reported.

Statistical analyses were performed using the Mixed Procedure in SAS (SAS Institute) with REML estimation and Type III tests of fixed effects. Outliers were assessed as those observations with standardized residuals greater than |3|. This resulted in one individual being removed from the *Ct.Ar* analysis, and two individuals removed from the *Tt.Ar* analysis. Selected (HR) mice and mice with wheel access were predicted to exhibit greater *Ct.Ar*, *Tt.Ar*, *J*, *Z<sub>p</sub>*, and robusticity indices than control mice and those without wheel access. One-tailed tests of significance were performed for linetype and activity (for which we had a priori directional predictions), while two-tailed tests were performed for linetype\*activity, the mini-muscle phenotype, and body mass (for which we did not have a priori predictions of group differences). Level of statistical significance was set at  $\alpha < 0.05$ .

### 3 | RESULTS

The relatively elongate mouse caudal ilium resembles a long bone in cross-section, with relatively thick cortical bone, a large medullary cavity, and few trabecular struts (Figure 1d). Control mice exhibit absolutely larger cross-sectional geometric properties than HR mice (Table 1). Results of the mixed model ANCOVAs show that ilium cross-sectional properties covary with body mass and that the mini-muscle phenotype has a significant effect on all cross-sectional properties except for total area robusticity index (Table 2). Linetype (HR versus control) did not have a significant effect on cross-sectional properties. Activity (wheel access versus no wheel access) had a statistically significant effect, increasing cortical area ( $p = .0471$ ) and its associated robusticity index ( $p = .0350$ ), as predicted (Tables 2 and 3, Figure 2). Activity also tended to increase values for all other measured and calculated traits, but these effects did not reach statistical significance (Tables 2 and 3). The interaction of linetype\*activity was not statistically significant (Table 2).

### 4 | DISCUSSION

Establishing relationships between physical activity and bone morphology by experimental manipulation in primates is not feasible because of their slow life-histories, relatively large body size, and sociability requirements. Here, we used a mouse model to test hypotheses relating ilium cross-sectional properties to physical activity, with the

**TABLE 1** Summary statistics (simple means and standard deviations) for cross-sectional geometric properties

Cross-sectional property	C, no wheel			C, wheel			HR, no wheel			HR, wheel			HR mini-muscle, wheel		
	N	Mean	SD	N	Mean	SD	N	Mean	SD	N	Mean	SD	N	Mean	SD
<i>Ct.Ar</i> , cortical area (mm <sup>2</sup> )	19	0.684	0.090	20	0.702	0.099	8	0.637	0.08	8	0.54	0.073	8	0.537	0.071
<i>Tt.Ar</i> , total periosteal area (mm <sup>2</sup> )	19	1.003	0.088	19	0.979	0.098	8	0.914	0.127	8	0.851	0.071	8	0.844	0.082
<i>Z<sub>p</sub></i> , polar section modulus (mm <sup>3</sup> )	19	0.216	0.031	20	0.213	0.034	9	0.189	0.04	8	0.161	0.023	8	0.158	0.026
<i>J</i> , polar moment of area (mm <sup>4</sup> )	19	0.152	0.029	20	0.151	0.031	9	0.129	0.034	8	0.104	0.019	8	0.103	0.021
<i>Ct.Ar</i> <sup>1/2</sup> /IL robusticity index	19	0.156	0.008	20	0.158	0.010	9	0.146	0.014	8	0.139	0.011	8	0.144	0.012
<i>Tt.Ar</i> <sup>1/2</sup> /IL robusticity index	19	0.189	0.010	20	0.188	0.008	9	0.179	0.015	8	0.175	0.011	8	0.180	0.011

C = Control, HR = High runner.



**TABLE 2** Results of mixed model ANCOVA. *p*-values listed for tests of main effects (linetype, HR vs. control, one-tailed; activity, wheel access vs no wheel access, one-tailed; the interaction between linetype and activity, two-tailed; mini-muscle phenotype, two-tailed; and body mass, two-tailed). Degrees of freedom (df) 1, 5 for all tests except for mini-muscle and body mass (where df are listed in parentheses)

Cross-sectional property	N	Linetype	Activity	Linetype*activity	Mini muscle	Body mass
Ct.Ar, cortical area (mm <sup>2</sup> )	73	0.3563	<b>0.0471</b>	0.1510	<b>&lt;0.0001</b> (1,56)	<b>&lt;0.0001</b> (1,56)
Tt.Ar, total periosteal area (mm <sup>2</sup> )	72	0.4083	0.0770	0.6776	<b>0.0097</b> (1,55)	<b>&lt;0.0001</b> (1,55)
Z <sub>p</sub> , polar section modulus (mm <sup>3</sup> )	74	0.2658	0.1040	0.7227	<b>0.0070</b> (1,57)	<b>&lt;0.0001</b> (1,57)
J, polar moment of area (mm <sup>4</sup> )	74	0.2463	0.1017	0.5406	<b>0.0148</b> (1,57)	<b>&lt;0.0001</b> (1,57)
Ct.Ar <sup>1/2</sup> /IL robusticity index	74	0.4091	<b>0.0175</b>	0.6246	<b>0.0262</b> (1,57)	<b>&lt;0.0001</b> (1,57)
Tt.Ar <sup>1/2</sup> /IL robusticity index	74	0.4893	0.0521	0.3489	0.1106 (1,57)	<b>&lt;0.0001</b> (1,57)

Bold denotes significance at  $\alpha < 0.05$ .

**TABLE 3** Least-squares means and standard errors from ANCOVA analyses shown in Table 2

Cross-sectional property	C, no wheel		C, wheel		HR, no wheel		HR, wheel		Nonmini-muscle		Mini-muscle	
	LS mean	SE	LS mean	SE	LS mean	SE	LS mean	SE	LS mean	SE	LS mean	SE
Ct.Ar, cortical area (mm <sup>2</sup> )	0.605	0.027	0.647	0.026	0.611	0.024	0.615	0.025	0.672	0.017	0.567	0.025
Tt.Ar, total periosteal area (mm <sup>2</sup> )	0.917	0.028	0.933	0.027	0.904	0.025	0.930	0.026	0.958	0.017	0.885	0.027
Z <sub>p</sub> , polar section modulus (mm <sup>3</sup> )	0.188	0.010	0.197	0.010	0.181	0.009	0.186	0.009	0.202	0.006	0.174	0.009
J, polar moment of area (mm <sup>4</sup> )	0.128	0.009	0.137	0.009	0.123	0.008	0.126	0.008	0.140	0.005	0.118	0.009
Ct.Ar <sup>1/2</sup> /IL robusticity index	0.149	0.005	0.154	0.005	0.147	0.004	0.153	0.005	0.156	0.003	0.146	0.004
Tt.Ar <sup>1/2</sup> /IL robusticity index	0.182	0.004	0.184	0.004	0.180	0.004	0.186	0.004	0.187	0.003	0.180	0.004

C = Control; HR = High runner.

aim to establish a foundation of data on which primate-specific hypotheses can be generated. To our knowledge, this study is the first to show that the mouse caudal ilium is beam-like and morphologically resembles a long bone in cross-section, with thick cortex, a large medullary cavity, and negligible trabecular struts. To test the hypothesis that mice bred for increased wheel-running activity (HR mice) have relatively stronger ilia than less active control mice, we analyzed cross-sectional geometric properties of the ilium. Ilium compressive (Ct.Ar), torsional (J), and bending strengths (Z<sub>p</sub>) were calculated, and

two robusticity indices were used to evaluate cortical bone mass relative to bone segment length (Ct.Ar<sup>1/2</sup>/caudal ilium length and Tt.Ar<sup>1/2</sup>/caudal ilium length). Analysis of similar robusticity indices in primates has suggested that more robust ilia are associated with larger locomotor loads (Lewton, 2015a, 2015c). The data from this study do not support the predictions that HR mice (both mini-muscle and nonmini-muscle) have relatively stronger caudal ilia than control mice. Instead, most differences in ilium cross-sectional properties are significantly related to body mass and the mini-muscle phenotype (which is associated with decreased hindlimb muscle mass and a variety of other effects). Specifically, larger mice exhibit larger values of cross-sectional properties and mini-muscle mice have the smallest values of cross-sectional properties. Although it is beyond the scope of this study to focus on the effects of the mini-muscle phenotype on bone cross-sectional properties, given that the mini-muscle phenotype was favored by the selective breeding procedures, associated changes in the ilium of mice with the mini-muscle phenotype can be viewed as part of the adaptive responses of the HR lines, albeit only in two of the four lines (i.e., an example of multiple solutions, sensu Garland et al., 2011). Our prediction that increased physical activity increases ilium resistance to loading was supported; increased activity via chronic wheel access was statistically associated with cortical area and its robusticity index, resulting in a 3% increase in cortical area robusticity index in the control lines and a 4% increase in the HR lines (Figure 1). The association between cortical area and physical activity in both control and HR mice (including individuals with the mini-muscle phenotype) suggests that the ilium responds to increased loading by inducing osteogenesis. Examining this phenomenon in primates might be possible within strepsirrhines, which are a natural experiment of sorts, in which species vary in typical locomotor modes

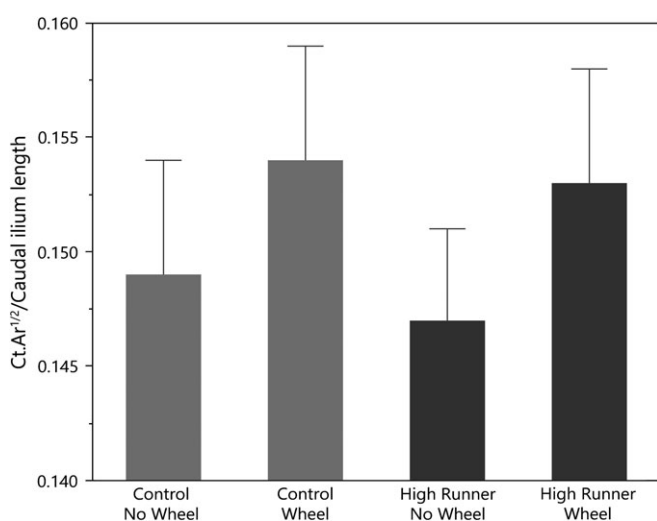


**FIGURE 2** Bar plot of least-squares means of the cortical area robusticity index by treatment group. Error bars are standard errors. The effect of chronic locomotor activity (wheel access) on robusticity index was statistically significant (1-tailed  $p = .0175$ ), but there was not a statistically significant effect of linetype, nor an interaction between linetype and activity (Table 2)

(e.g., arboreal quadrupedalism versus vertical clinging and leaping) and typical load magnitudes (i.e., vertical clingers and leapers experience substrate reaction forces orders of magnitude larger than their quadrupedal counterparts, [Demes, Fleagle, & Jungers, 1999]).

Our results are broadly similar to previous studies on long bones of the HR mice that show an inconsistent effect of increased chronic wheel-running activity on bone cross-sectional properties. Neither femoral nor humeral midshaft cross-sectional properties demonstrated a statistically significant effect of activity in other studies of these particular mice (Copes et al., 2018) or those sampled from another generation (Middleton et al., 2010). Middleton et al. (2010) document some significant differences in femoral cross-sectional properties (maximum second moment of area and section modulus) by linetype, and also in relation to the mini-muscle phenotype, but none by activity. However, Wallace et al. (2012) document femoral diaphyseal differences by linetype (50% of examined traits significantly differed by linetype), the mini-muscle phenotype (17% of examined traits significantly differed by mini-muscle phenotype), and activity (33% of examined traits significantly differed by activity). Specifically, of the femoral diaphyseal cross-sectional properties analyzed by Wallace et al. (2012), only endocortical area (i.e., medullary cavity area) and cortical thickness differed according to whether they were housed with access to wheels. This result held when comparisons were examined within the HR linetype. Within the control linetype, an additional cross-sectional property—total (periosteal) area—differed according to activity (Wallace et al., 2012). Therefore, previous work examining bone cross-sectional geometry in HR mice has shown that activity and linetype have inconsistent effects on cross-sectional morphology, suggesting that the effects on bone cross-sectional geometry of genetic factors and activity levels within an individual's lifetime are complex and not well understood.

A limitation of this study is the assumption that increased wheel-running activity would result in bone deposition in this sample of females. In contrast, it is possible that repetitive loading and/or magnitudes of loads were not sufficiently great and/or frequent enough to warrant increased bone mass or changes in cortical bone distribution. This seems unlikely, at least for mice from the selectively bred HR lines, as they ran very substantial distances for 3 months, including during the juvenile period from weaning to sexual maturity (Copes et al., 2018), which is a critical period for bone development (Pearson & Lieberman, 2004; Ruff, Holt, & Trinkaus, 2006). Of mice with access to wheels, HR mice ran significantly farther, longer, and faster than control mice (all  $p < .03$ , see Copes et al., 2015). Of mice without access to wheels, total home cage activity was 1.5 times greater in HR mice than in control mice ( $p = .0078$ , see Copes et al., 2015). Another possibility is that the mice that resulted from this artificial selection experiment might not be particularly responsive to loading. Indeed, previous studies of inbred strains of mice have shown differences in their responsiveness to mechanical loading and/or wheel access (Jepsen, Akkus, Majeska, & Nadeau, 2003; Kesavan, Mohan, Oberholtzer, Wergedal, & Baylink, 2005; Kodama et al., 2000; Robling & Turner, 2002; Turner et al., 2000). Lastly, given the relatively small body mass of mice and the potential for scaling differences in bone cross-sectional geometry across mammals of varying size, perhaps mouse long bones should not be expected to respond to loading as

would those of a larger-bodied mammal. Indeed, Wallace et al. (2012) suggest that mice may require relatively greater bone stress to induce bone remodeling. This hypothesis is corroborated by experimental work demonstrating that cortical bone osteogenesis in the mouse tibia is dose-dependent and requires peak strains that are greater than those encountered during normal locomotion (Berman, Clauser, Wunderlin, Hammond, & Wallace, 2015; De Souza et al., 2005; Weatherholt, Fuchs, & Warden, 2013).

In summary, these data only marginally support the hypothesis that increased physical activity strengthens the caudal ilium. The next reasonable step to determine how loading affects the caudal ilium may be to alter the load magnitudes encountered to assess whether relatively large loads result in strengthened caudal ilia as evidenced by alterations in cross-sectional properties. In mice, this might be accomplished by jumping (Kodama et al., 2000; Umemura, Baylink, Wergedal, Mohan, & Srivastava, 2002) or climbing exercise (Green et al., 2012; Lionikas & Blizard, 2008; Mori et al., 2003). Although extrapolating from small-bodied mice to primates that vary in body size from relatively small to large warrants caution due to such biological differences as the scaling of bone microstructure (Barak, Lieberman, & Hublin, 2013), our study suggests that properties of cortical bone in the primate caudal ilium could be related to loading regimes experienced by individuals during their lifetime and hence could differ among species that use different positional behaviors. Although the ultimate causes of potential primate species differences in bone morphology are difficult to determine (i.e., evolved differences versus bone functional adaptation), the observable relationship between caudal ilium morphology and loading regimes is testable in primates.

## ACKNOWLEDGMENTS

We thank Fettah Kosar for training KLL on the use of the  $\mu$ CT scanner at Harvard University's Center for Nanoscale Systems, and Tim Ryan for useful discussion on data processing. We thank the Associate Editor and reviewers for their useful comments, which have strengthened the manuscript. Supported by US NSF grants IOS-11212732 (TG), DEB-1655362 (TG), and DDIG 0925793 (LC), and Wenner-Gren Foundation Dissertation Grant Number: 8102 (LC).

## ORCID

Kristi L. Lewton  <https://orcid.org/0000-0003-0674-2454>

Lynn E. Copes  <https://orcid.org/0000-0002-4337-4016>

## REFERENCES

- Anderson, A. E., Peters, C. L., Tuttle, B. D., & Weiss, J. A. (2005). Subject-specific finite element model of the pelvis: Development, validation and sensitivity studies. *Journal of Biomechanical Engineering*, 127(3), 364–373. <https://doi.org/10.1115/1.1894148>
- Barak, M. M., Lieberman, D. E., & Hublin, J.-J. (2013). Of mice, rats and men: Trabecular bone architecture in mammals scales to body mass with negative allometry. *Journal of Structural Biology*, 183(2), 123–131. <https://doi.org/10.1016/j.jsb.2013.04.009>
- Berman, A. G., Clauser, C. A., Wunderlin, C., Hammond, M. A., & Wallace, J. M. (2015). Structural and mechanical improvements to bone are strain dependent with axial compression of the tibia in female C57BL/6 mice. *PLoS One*, 10(6), e0130504. <https://doi.org/10.1371/journal.pone.0130504>

- Burr, D. B., Piotrowski, G., Martin, R. B., & Cook, P. N. (1982). Femoral mechanics in the lesser bushbaby (*Galago senegalensis*): Structural adaptations to leaping in primates. *The Anatomical Record*, 202(3), 419–429. <https://doi.org/10.1002/ar.1092020314>
- Burr, D. B., Ruff, C. B., & Johnson, C. (1989). Structural adaptations of the femur and humerus to arboreal and terrestrial environments in three species of macaque. *American Journal of Physical Anthropology*, 79(3), 357–367. <https://doi.org/10.1002/ajpa.1330790312>
- Carlson, K. J. (2005). Investigating the form-function interface in African apes: Relationships between principal moments of area and positional behaviors in femoral and humeral diaphyses. *American Journal of Physical Anthropology*, 127(3), 312–334. <https://doi.org/10.1002/ajpa.20124>
- Carlson, K. J., & Marchi, D. (Eds.). (2014). *Reconstructing mobility: Environmental, behavioral, and morphological determinants*. New York: Springer.
- Carter, D. R., Vasu, R., & Harris, W. H. (1982). Stress distributions in the acetabular region—II. Effects of cement thickness and metal backing of the total hip acetabular component. *Journal of Biomechanics*, 15(3), 165–170.
- Castro, A. A., & Garland, T., Jr. (2018). Evolution of hindlimb bone dimensions and muscle masses in house mice selectively bred for high voluntary wheel-running behavior. *Journal of Morphology*, 279(6), 766–779. <https://doi.org/10.1002/jmor.20809>
- Copes, L. E., Schutz, H., Dlugosz, E. M., Acosta, W., Chappell, M. A., & Garland, T., Jr. (2015). Effects of voluntary exercise on spontaneous physical activity and food consumption in mice: Results from an artificial selection experiment. *Physiology & Behavior*, 149, 86–94. <https://doi.org/10.1016/j.physbeh.2015.05.025>
- Copes, L. E., Schutz, H., Dlugosz, E. M., Judex, S., & Garland, T., Jr. (2018). Locomotor activity, growth hormones, and systemic robusticity: An investigation of cranial vault thickness in mouse lines bred for high endurance running. *American Journal of Physical Anthropology*, 166(2), 442–458. <https://doi.org/10.1002/ajpa.23446>
- Dalstra, M., & Huiskes, R. (1995). Load transfer across the pelvic bone. *Journal of Biomechanics*, 28(6), 715–724.
- Dalstra, M., Huiskes, R., & van Erning, L. (1995). Development and validation of a three-dimensional finite element model of the pelvic bone. *Journal of Biomechanical Engineering*, 117(3), 272–278.
- De Souza, R. L., Matsuura, M., Eckstein, F., Rawlinson, S. C. F., Lanyon, L. E., & Pitsillides, A. A. (2005). Non-invasive axial loading of mouse tibiae increases cortical bone formation and modifies trabecular organization: A new model to study cortical and cancellous compartments in a single loaded element. *Bone*, 37(6), 810–818. <https://doi.org/10.1016/j.bone.2005.07.022>
- Demes, B., Fleagle, J. G., & Jungers, W. L. (1999). Takeoff and landing forces of leaping strepsirrhine primates. *Journal of Human Evolution*, 37, 279–292.
- Demes, B., & Jungers, W. L. (1993). Long bone cross-sectional dimensions, locomotor adaptations and body size in prosimian primates. *Journal of Human Evolution*, 25, 57–74.
- Demes, B., Qin, Y. X., Stern, J. T., Larson, S. G., & Rubin, C. T. (2001). Patterns of strain in the macaque tibia during functional activity. *American Journal of Physical Anthropology*, 116(4), 257–265. <https://doi.org/10.1002/ajpa.1122>
- Demes, B., Stern, J. T., Hausman, M. R., Larson, S. G., McLeod, K. J., & Rubin, C. T. (1998). Patterns of strain in the macaque ulna during functional activity. *American Journal of Physical Anthropology*, 106(1), 87–100. [https://doi.org/10.1002/\(SICI\)1096-8644\(199805\)106:1<87::AID-AJPA6>3.0.CO;2-A](https://doi.org/10.1002/(SICI)1096-8644(199805)106:1<87::AID-AJPA6>3.0.CO;2-A)
- Doube, M., Kłosowski, M. M., Arganda-Carreras, I., Cordelières, F. P., Dougherty, R. P., Jackson, J. S., ... Shefelbine, S. J. (2010). BoneJ: Free and extensible bone image analysis in ImageJ. *Bone*, 47(6), 1076–1079. <https://doi.org/10.1016/j.bone.2010.08.023>
- Finlay, J. B., Bourne, R. B., Landsberg, R. P. D., & Andreae, P. (1986). Pelvic stresses in vitro—I. Malsizing of endoprostheses. *Journal of Biomechanics*, 19, 703–714.
- Garland, T., Jr. (2003). Selection experiments: An under-utilized tool in biomechanics and organismal biology. In V. L. Bels, J. P. Gasc, & A. Casino (Eds.), *Vertebrate biomechanics and evolution* (pp. 23–56). Oxford: BIOS Scientific Publishers.
- Garland, T., Jr., Kelly, S. A., Malisch, J. L., Kolb, E. M., Hannon, R. M., Keeney, B. K., ... Middleton, K. M. (2011). How to run far: Multiple solutions and sex-specific responses to selective breeding for high voluntary activity levels. *Proceedings of the Royal Society B*, 278(1705), 574–581. <https://doi.org/10.1098/rspb.2010.1584>
- Garland, T., Jr., Morgan, M. T., Swallow, J. G., Rhodes, J. S., Girard, I., Belter, J. G., & Carter, P. A. (2002). Evolution of a small-muscle polymorphism in lines of house mice selected for high activity levels. *Evolution*, 56(6), 1267–1275.
- Green, D. J., Richmond, B. G., & Miran, S. L. (2012). Mouse shoulder morphology responds to locomotor activity and the kinematic differences of climbing and running. *Journal of Experimental Zoology. Part B, Molecular and Developmental Evolution*, 318(8), 621–638. <https://doi.org/10.1002/jez.b.22466>
- Huiskes, R. (1987). Finite element analysis of acetabular reconstruction. *Acta Orthopaedica Scandinavica*, 58, 620–625.
- Jepsen, K. J., Akkus, O. J., Majeska, R. J., & Nadeau, J. H. (2003). Hierarchical relationship between bone traits and mechanical properties in inbred mice. *Mammalian Genome*, 14(2), 97–104. <https://doi.org/10.1007/s00335-002-3045-y>
- Kelly, S. A., Bell, T. A., Selitsky, S. R., Buus, R. J., Hua, K., Weinstock, G. M., ... Pomp, D. (2013). A novel intronic single nucleotide polymorphism in the myosin heavy polypeptide 4 gene is responsible for the mini-muscle phenotype characterized by major reduction in hind-limb muscle mass in mice. *Genetics*, 195(4), 1385–1395. <https://doi.org/10.1534/genetics.113.154476>
- Kelly, S. A., Czech, P. P., Wight, J. T., Blank, K. M., & Garland, T., Jr. (2006). Experimental evolution and phenotypic plasticity of hindlimb bones in high-activity house mice. *Journal of Morphology*, 267(3), 360–374. <https://doi.org/10.1002/jmor.10407>
- Kesavan, C., Mohan, S., Oberholzer, S., Wergedal, J. E., & Baylink, D. J. (2005). Mechanical loading-induced gene expression and BMD changes are different in two inbred mouse strains. *Journal of Applied Physiology*, 99(5), 1951–1957. <https://doi.org/10.1152/japplphysiol.00401.2005>
- Kodama, Y., Umemura, Y., Nagasawa, S., Beamer, W. G., Donahue, L. R., Rosen, C. R., ... Farley, J. R. (2000). Exercise and mechanical loading increase periosteal bone formation and whole bone strength in C57BL/6J mice but not in C3H/HeJ mice. *Calcified Tissue International*, 66(4), 298–306.
- Lewton, K. L. (2015a). Allometric scaling and locomotor function in the primate pelvis. *American Journal of Physical Anthropology*, 156(4), 511–530. <https://doi.org/10.1002/ajpa.22696>
- Lewton, K. L. (2015b). In vitro bone strain distributions in a sample of primate pelves. *Journal of Anatomy*, 226(5), 458–477. <https://doi.org/10.1111/joa.12294>
- Lewton, K. L. (2015c). Pelvic form and locomotor adaptation in strepsirrhine primates. *Anatomical Record*, 298(1), 230–248. <https://doi.org/10.1002/ar.23070>
- Lieberman, D. E., & Pearson, O. M. (2001). Trade-off between modeling and remodeling responses to loading in the mammalian limb. *Bulletin of the Museum of Comparative Zoology at Harvard College*, 156, 269–282.
- Lieberman, D. E., Polk, J. D., & Demes, B. (2004). Predicting long bone loading from cross-sectional geometry. *American Journal of Physical Anthropology*, 123(2), 156–171. <https://doi.org/10.1002/ajpa.10316>
- Linstrom, N. J., Heiserman, J. E., Kortman, K. E., Crawford, N. R., Baek, S., Anderson, R. L., ... Dean, B. L. (2009). Anatomical and biomechanical analyses of the unique and consistent locations of sacral insufficiency fractures. *Spine*, 34(4), 309–315. <https://doi.org/10.1097/BRS.0b013e318191ea01>
- Lionberger, D., Walker, P. S., & Granholm, J. (1985). Effects of prosthetic acetabular replacement on strains in the pelvis. *Journal of Orthopaedic Research*, 3(3), 372–379. <https://doi.org/10.1002/jor.1100030314>
- Lionikas, A., & Blizard, D. A. (2008). Diverse effects of stanozolol in C57BL/6J and a/J mouse strains. *European Journal of Applied Physiology*, 103(3), 333–341. <https://doi.org/10.1007/s00421-008-0708-8>
- Marchi, D. (2007). Relative strength of the tibia and fibula and locomotor behavior in hominoids. *Journal of Human Evolution*, 53(6), 647–655. <https://doi.org/10.1016/j.jhevol.2007.05.007>
- Middleton, K. M., Goldstein, B. D., Guduru, P. R., Waters, J. F., Kelly, S. A., Swartz, S. M., & Garland, T., Jr. (2010). Variation in within-bone



- stiffness measured by nanoindentation in mice bred for high levels of voluntary wheel running. *Journal of Anatomy*, 216(1), 121–131. <https://doi.org/10.1111/j.1469-7580.2009.01175.x>
- Middleton, K. M., Kelly, S. A., & Garland, T., Jr. (2008). Selective breeding as a tool to probe skeletal response to high voluntary locomotor activity in mice. *Integrative and Comparative Biology*, 48(3), 394–410. <https://doi.org/10.1093/icb/icn057>
- Misof, B. M., Dempster, D. W., Zhou, H., Roschger, P., Fratzl-Zelman, N., Fratzl, P., ... Klaushofer, K. (2014). Relationship of bone mineralization density distribution (BMDD) in cortical and cancellous bone within the iliac crest of healthy premenopausal women. *Calcified Tissue International*, 95(4), 332–339. <https://doi.org/10.1007/s00223-014-9901-4>
- Mori, T., Okimoto, N., Sakai, A., Okazaki, Y., Nakura, N., Notomi, T., & Nakamura, T. (2003). Climbing exercise increases bone mass and trabecular bone turnover through transient regulation of marrow osteogenic and osteoclastogenic potentials in mice. *Journal of Bone and Mineral Research*, 18(11), 2002–2009. <https://doi.org/10.1359/jbmr.2003.18.11.2002>
- Patel, B. A., Ruff, C. B., Simons, E. L. R., & Organ, J. M. (2013). Humeral cross-sectional shape in suspensory primates and sloths. *Anatomical Record*, 296(4), 545–556. <https://doi.org/10.1002/ar.22669>
- Peacock, S. J., Garland, T., Jr., & Middleton, K. M. (2018). Reply to Ruff, Warden, and Karlson. *American Journal of Physical Anthropology*, 167(1), 190–193. <https://doi.org/10.1002/ajpa.23614>
- Pearson, O. M. (2000). Activity, climate, and postcranial robusticity: Implications for modern human origins and scenarios of adaptive change. *Current Anthropology*, 41, 569–589.
- Pearson, O. M., & Lieberman, D. E. (2004). The aging of Wolff's "law": Ontogeny and responses to mechanical loading in cortical bone. *American Journal of Physical Anthropology*, 125(Suppl 39), 63–99. <https://doi.org/10.1002/ajpa.20155>
- Ries, M., Pugh, J., Au, J. C., Gurtowski, J., & Dee, R. (1989). Normal pelvic strain pattern in vitro. *Journal of Biomedical Engineering*, 11(5), 398–402.
- Robling, A. G., & Turner, C. H. (2002). Mechanotransduction in bone: Genetic effects on mechanosensitivity in mice. *Bone*, 31(5), 562–569.
- Roschger, P., Paschalis, E. P., Fratzl, P., & Klaushofer, K. (2008). Bone mineralization density distribution in health and disease. *Bone*, 42(3), 456–466. <https://doi.org/10.1016/j.bone.2007.10.021>
- Ruff, C., Holt, B., & Trinkaus, E. (2006). Who's afraid of the big bad Wolff?: "Wolff's law" and bone functional adaptation. *American Journal of Physical Anthropology*, 129(4), 484–498. <https://doi.org/10.1002/ajpa.20371>
- Ruff, C. B. (2002). Long bone articular and diaphyseal structure in old world monkeys and apes. I: Locomotor effects. *American Journal of Physical Anthropology*, 119(4), 305–342. <https://doi.org/10.1002/ajpa.10117>
- Ruff, C. B. (2003). Long bone articular and diaphyseal structure in Old World monkeys and apes. II: Estimation of body mass. *American Journal of Physical Anthropology*, 120(1), 16–37. <https://doi.org/10.1002/ajpa.10118>
- Ruff, C. B., & Hayes, W. C. (1983). Cross-sectional geometry of Pecos Pueblo femora and tibiae—a biomechanical investigation: II. Sex, age, side differences. *American Journal of Physical Anthropology*, 60(3), 383–400. <https://doi.org/10.1002/ajpa.1330600309>
- Schaffler, M. B., Burr, D. B., Jungers, W. L., & Ruff, C. B. (1985). Structural and mechanical indicators of limb specialization in primates. *Folia Primatologica; International Journal of Primatology*, 45, 61–75.
- Schneider, C. A., Rasband, W. S., & Eliceiri, K. W. (2012). NIH image to ImageJ: 25 years of image analysis. *Nature Methods*, 9(7), 671–675.
- Schutz, H., Jamniczky, H. A., Hallgrímsson, B., & Garland, T., Jr. (2014). Shape-shift: Semicircular canal morphology responds to selective breeding for increased locomotor activity. *Evolution*, 68(11), 3184–3198. <https://doi.org/10.1111/evo.12501>
- Schwartz, N. L., Patel, B. A., Garland, T., Jr., & Horner, A. M. (2018). Effects of selective breeding for high voluntary wheel-running behavior on femoral nutrient canal size and abundance in house mice. *Journal of Anatomy*, 233(2), 193–203. <https://doi.org/10.1111/joa.12830>
- Shaw, C. N., & Stock, J. T. (2009). Intensity, repetitiveness, and directionality of habitual adolescent mobility patterns influence the tibial diaphysis morphology of athletes. *American Journal of Physical Anthropology*, 140(1), 149–159. <https://doi.org/10.1002/ajpa.21064>
- Shim, V. B., Pitto, R. P., Streicher, R. M., Hunter, P. J., & Anderson, I. A. (2007). The use of sparse CT datasets for auto-generating accurate FE models of the femur and pelvis. *Journal of Biomechanics*, 40(1), 26–35. <https://doi.org/10.1016/j.jbiomech.2005.11.018>
- Stock, J., & Pfeiffer, S. (2001). Linking structural variability in long bone diaphyses to habitual behaviors: Foragers from the southern African later stone age and the Andaman Islands. *American Journal of Physical Anthropology*, 115(4), 337–348. <https://doi.org/10.1002/ajpa.1090>
- Swallow, J. G., Carter, P. A., & Garland, T., Jr. (1998). Artificial selection for increased wheel-running behavior in house mice. *Behavior Genetics*, 28(3), 227–237.
- Terranova, C. J. (1995a). Functional morphology of leaping behaviors in galagids: Associations between landing limb use and diaphyseal geometry. In L. Alterman, G. A. Doyle, & M. K. Izard (Eds.), *Creatures of the dark: The nocturnal prosimians* (pp. 473–493). New York: Plenum Press.
- Terranova, C. J. (1995b). Leaping behaviors and the functional morphology of strepsirrhine primate long bones. *Folia Primatologica; International Journal of Primatology*, 65, 181–201.
- Trinkaus, E., & Churchill, S. E. (1999). Diaphyseal cross-sectional geometry of near eastern middle Palaeolithic humans: The Humerus. *Journal of Archaeological Science*, 26(2), 173–184. <https://doi.org/10.1006/jasc.1998.0314>
- Trinkaus, E., Ruff, C. B., Churchill, S. E., & Vandermeersch, B. (1998). Locomotion and body proportions of the Saint-Césaire 1 Châtelperronian Neandertal. *Proceedings of the National Academy of Sciences of the United States of America*, 95, 5836–5840.
- Turner, C. H., Hsieh, Y. F., Müller, R., Bouxsein, M. L., Baylink, D. J., Rosen, C. J., ... Beamer, W. G. (2000). Genetic regulation of cortical and trabecular bone strength and microstructure in inbred strains of mice. *Journal of Bone and Mineral Research*, 15(6), 1126–1131. <https://doi.org/10.1359/jbmr.2000.15.6.1126>
- Umemura, Y., Baylink, D. J., Wergedal, J. E., Mohan, S., & Srivastava, A. K. (2002). A time course of bone response to jump exercise in C57BL/6J mice. *Journal of Bone and Mineral Metabolism*, 20(4), 209–215. <https://doi.org/10.1007/s007740200030>
- Wallace, I. J., & Garland, T., Jr. (2016). Mobility as an emergent property of biological organization: Insights from experimental evolution. *Evolutionary Anthropology*, 25(3), 98–104. <https://doi.org/10.1002/evan.21481>
- Wallace, I. J., Middleton, K. M., Lublinsky, S., Kelly, S. A., Judex, S., Garland, T., Jr., & Demes, B. (2010). Functional significance of genetic variation underlying limb bone diaphyseal structure. *American Journal of Physical Anthropology*, 143(1), 21–30. <https://doi.org/10.1002/ajpa.21286>
- Wallace, I. J., Tommasini, S. M., Judex, S., Garland, T., Jr., & Demes, B. (2012). Genetic variations and physical activity as determinants of limb bone morphology: An experimental approach using a mouse model. *American Journal of Physical Anthropology*, 148(1), 24–35. <https://doi.org/10.1002/ajpa.22028>
- Weatherholt, A. M., Fuchs, R. K., & Warden, S. J. (2013). Cortical and trabecular bone adaptation to incremental load magnitudes using the mouse tibial axial compression loading model. *Bone*, 52(1), 372–379. <https://doi.org/10.1016/j.bone.2012.10.026>

**How to cite this article:** Lewton KL, Ritzman T, Copes LE, Garland Jr T, Capellini TD. Exercise-induced loading increases ilium cortical area in a selectively bred mouse model. *Am J Phys Anthropol*. 2019;168:543–551. <https://doi.org/10.1002/ajpa.23770>